



From the journal:
Physical Chemistry Chemical Physics

Stabilization of electrogenerated copper species on electrodes modified with quantum dots



[Daniel Martín-Yerga](#)^a and [Agustín Costa-García](#)^{*a}

⊖ [Author affiliations](#)

* Corresponding authors

^a Departamento de Química Física y Analítica, Universidad de Oviedo, Julián Clavería 8, 33006 Oviedo, Spain

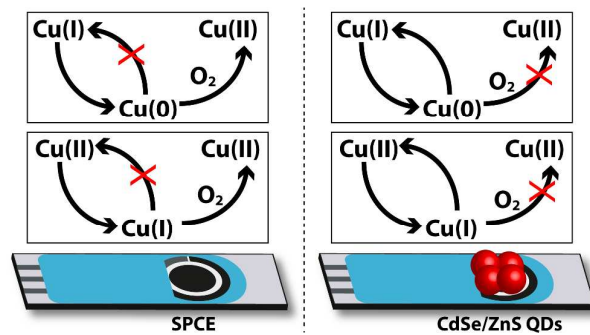
E-mail: costa@uniovi.es

Tel: +34 985103486

This is a preprint manuscript. Please, download the final and much nicer version at:

<https://doi.org/10.1039/C6CP07957A>

TOC GRAPHICS



Electrogenerated Cu(I) and Cu(0) species are stabilized by quantum dots at modified electrodes

Stabilization of Electrogenerated Copper Species on Electrodes Modified with Quantum Dots

*Daniel Martín-Yerga and Agustín Costa-García**

Departamento de Química Física y Analítica, Universidad de Oviedo, 33006 Oviedo, Spain.

* Corresponding author: Prof. Dr. Agustín Costa García

Departamento de Química Física y Analítica

Universidad de Oviedo

Julián Clavería 8, Oviedo 33006 (Spain)

E-mails: costa@uniovi.es

Telephone: (+34) 985103486

ABSTRACT

Quantum dots have special optical, surface and electronic properties that can be used for electrochemical applications. In this work, the electrochemical behavior of copper in ammonia medium is described using bare screen-printed carbon electrodes and modified with CdSe/ZnS quantum dots. At bare electrodes, the electro-generated Cu(I) and Cu(0) species are oxidized by dissolved oxygen in a fast coupled chemical reaction. At quantum dots-modified electrodes, the re-oxidation of Cu(I) and Cu(0) species can be observed, which indicates that they are stabilized by the nanocrystals present on the electrode surface. A weak adsorption is proposed as the main cause for the stabilization. The electrodeposition on electrodes modified with quantum dots allows the generation of random nanostructures with copper nanoparticles avoiding the preferential nucleation onto the most active electrode areas.

KEYWORDS: Quantum dots; Copper; Ammonia; Nanocrystal; Nanoparticle

1. INTRODUCTION

Quantum dots (QDs) are semiconductor nanoparticles with size within a few nm and crystal structure¹. They have special optical, electronic and surface properties due to their high surface/volume ratio and the quantum confinement^{2,3}. Their most abundant applications have been taking advantage of the luminescent features, such as in optical devices or solar cells⁴ or bioassays⁵. QDs on electrodes have been used to study their electronic properties^{6,7}, for photoelectrochemical or electrochemiluminescent applications^{8,9}, for improving transduction^{10,11} or as label for electrochemical biosensors^{12,13}. The special properties of QDs have led to study their interaction with many species such as metal ions, approach that can be used for analytical detection^{14,15} or even for the synthesis of new nanocrystals by cationic exchange¹⁶⁻¹⁸. In this regard, recently, we have described the selective electrodeposition of silver on the surface of QDs attached to electrodes¹⁹. When QDs-modified electrodes are used, silver reduction is carried out catalytically, at a more positive potential than for carbon electrodes. A strong adsorption of elemental silver on the QDs surface was also observed. Therefore, the study of the electrochemical behavior of metal cations at electrodes modified with QDs can provide information about new properties and applications of these nanoparticles.

Electrochemistry of copper has been extensively studied because its importance in various industrial processes. For instance, cupric species in ammonia are used for etching copper in the manufacture of printed circuit boards, a process which is carried out by redox reactions^{20,21}. Corrosion/dissolution of elemental copper in ammonia media has also been widely described²²⁻²⁵ because it is a material frequently used for industrial or domestic applications. Finally, copper electrodeposition, a process which can be used to manufacture materials coated with copper films, has also been extensively studied²⁶⁻³⁰. Interesting information was obtained from the examination of the electrochemical behavior of copper in ammonia from all these kind of studies, such as that oxygen in solution could be able to dissolve elemental copper at high rates under certain

conditions^{24,25} or the oxidation of Cu(I) species also by oxygen^{20,21}. However, most of these works described the electrochemical behavior of copper using high concentrations, typically above the mM range. Therefore, the influence of oxygen could be neglected because its concentration is in defect with respect to the concentration of copper. It would be interesting to study the electrochemical behavior of copper in ammonia with small copper concentrations, where the reaction with oxygen may have a significant effect.

By combining both topics, in this paper, we study the electrochemical behavior of copper in ammonia using initial low Cu(II) concentrations with screen-printed carbon electrodes. This way, we are able to study the effect of the possible reactions of copper with oxygen. Then, we study the electrochemical behavior of copper under the same conditions but using electrodes modified with CdSe/ZnS quantum dots, which leads to a quite different response due to the special properties of the quantum dots.

2. MATERIALS AND METHODS

2.1. Apparatus and electrodes

Electrochemical measurements were conducted with μ Stat 8000 (DropSens) potentiostat/galvanostat interfaced to an Apple Macbook Air laptop and controlled by the DropView 8400 2.2 software. 8-channel screen-printed electrochemical arrays (SPCEs) were purchased from DropSens (ref. 8x110). Each array is formed by eight 3-electrode electrochemical cells with carbon-based working and counter electrodes, whereas quasireference electrodes and electric contacts are made of silver. This device has dimensions of 4.0 x 7.9 x 0.06 cm (length x width x height) and the diameter of the circular working electrode is 2.56 mm. 8-channel arrays were connected to the potentiostat through a specific connector, DRP-CAST8x. All measurements were carried out at room temperature and using an aliquot of 25 μ L of the appropriate solution. All reported potentials are versus the silver quasireference screen-printed electrode. A JEOL 6610LV

scanning electron microscope (SEM) was used to characterize the working electrodes after the electrodeposition of copper. ImageJ software was used for estimation of nanoparticle size in the SEM images.

2.2. Reagents and solutions

Ammonia solution (25%), sulfuric acid (98%), sodium dithionite and fuming hydrochloric acid were purchased from Merck. Copper nitrate trihydrate and tris(hydroxymethyl)aminomethane (Tris) were purchased from Sigma-Aldrich. CdSe/ZnS Qdot® 655 Biotin Conjugate (QDs) was purchased from Life Technologies. Ultrapure water obtained with a Millipore Direct Q5™ purification system from Millipore Ibérica S.A. (Madrid, Spain) was used throughout this work. All other reagents were of analytical grade. Working solutions of QDs were prepared in 0.1 M pH 7.4 Tris-HCl buffer, as they are stable in this solution. Unless stated otherwise, 4 μL of a 5 nM solution of QDs were employed for the modification of electrodes. QDs concentration is always given as particle concentration. Cu(II) solutions were prepared in 1 M NH_3 aqueous solution (pH 11.5). NH_3 solution is essential in order to have soluble copper ions and an alkaline media, where the QDs are stable. For measurements in absence of O_2 using screen-printed electrodes, the solutions were firstly saturated with N_2 , and a small amount (50 μM) of sodium dithionite was added in order to reduce the last traces of oxygen. As an excess of dithionite could also reduce part of the Cu(II), a potential of +0.8 V for 30 s was applied before the oxygen-free measurements in order to oxidize all the copper in solution.

3. RESULTS AND DISCUSSION

We first report the electrochemistry of copper in 1 M NH_3 at bare screen-printed electrodes and discuss the behavior found. Second, we discuss the electrochemistry of copper at quantum dots-modified screen-printed electrodes and a comparison between the behavior found in both electrodes is performed.

3.1. Electrochemistry of copper at bare screen-printed carbon electrodes

Figure 1A shows the voltammogram obtained for a 25 μM solution of Cu(II) in 1 M NH_3 measured at a scan rate of 50 mV/s using bare SPCEs. The potential was swept from +0.5 to -1.2 V (cathodic curve) and back to +0.5 V (anodic curve). Several processes can be observed in the cathodic and anodic curves. A decrease in the current can be observed at the cathodic curve with onset at a potential of -0.1 V. This process maintains a quasi-limiting current until approaching more negative potentials, and therefore, a peak-shaped response was not obtained. At a potential near -0.5 V the onset of a new cathodic process with a peak potential (E_p) around -0.65 V is observed, but it is overlapped with a larger cathodic process with E_p at -0.77 V. This last process is also observed with a E_p near -0.80 V at the voltammogram for the blank solution (1 M NH_3), which is also shown in the mentioned figure. It is attributed to the oxygen reduction reaction (ORR)³¹ due to the O_2 present in the solution. The other two cathodic processes are thus due to the copper species in solution. It is widely known³² that Cu(II) forms a complex in presence of excess NH_3 , which initially would be the species $[\text{Cu}(\text{NH}_3)_4]^{2+}$. Furthermore, in this medium Cu(I) species can be obtained after the reduction of Cu(II) due to the stabilization by the coordination sphere, forming typically $[\text{Cu}(\text{NH}_3)_2]^+$ or $[\text{Cu}(\text{NH}_3)_3]^+$ as described in the literature^{33,32}. It seems to be some ongoing discussion about the coordination sphere of these species and in order to simplify the notation, hereinafter these species will be abbreviated as Cu(II) and Cu(I). Therefore, the cathodic processes found at SPCEs can be assigned to the reduction of Cu(II) to Cu(I) at the more positive potential and the reduction of Cu(I) to Cu(0) at the most negative potential, besides the ORR already mentioned. Two anodic processes were observed, suggested by the increment of the anodic current at a potential near -0.4 V, and at a potential close to -0.1 V. These processes can be attributed to the oxidation of Cu(0) to Cu(I) and the oxidation of Cu(I) to Cu(II), respectively^{21,29}. The electrochemical response obtained is different to other previously published studies for copper

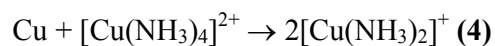
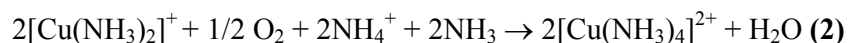
electrochemistry in ammonia-based media^{21,29}. In these studies, the processes observed are peak-shaped, although they were obtained with higher initial concentrations of Cu(II). New voltammograms were recorded with increasing concentrations of Cu(II) at SPCEs and are shown in **Figure S1**. For higher Cu(II) concentrations, the electrochemical processes are, generally, peak-shaped, whereas at lower concentrations, the processes are more similar to steady state curves. Furthermore, at low concentrations, the stripping process appears to occur as two different processes at a different potential, suggesting one of these two situations: copper is deposited in different distributions (perhaps forming a multilayer-like structure), or the stripping occurs in two different thermodynamic ways. For 250 μM and above, this process is observed as one stripping process, probably due to overlapping of the two stripping processes or due to that one of them is more significant at these concentrations.

[FIGURE 1]

The electrochemical behavior of copper under these conditions is especially interesting for the processes involving Cu(II)/Cu(I) at the most positive potentials, and they can be studied more clearly as no other overlapping processes appeared at these potentials. **Figure 1B** shows the voltammograms obtained for a 25 μM solution of Cu(II) in 1 M NH_3 measured at several scan rates (0.01-3 V/s) using bare SPCEs. In this case, the switching potential was -0.4 V, enough to study the redox processes involving the Cu(II)/Cu(I) species. At low scan rates, the cathodic response is a quasi-limiting current similar to that obtained for steady state voltammograms. In addition, the anodic process is diminished with current values near zero. The limiting current increases slightly with the scan rate, so the behavior is not entirely as a steady state voltammogram, since for these cases, the limiting current does not depend on the scan rate³⁴. Therefore, it appears that the mass transfer is much greater than for a typical diffusion-controlled process. At high scan rates (specially for 1 V/s and higher), the responses are peak-shaped, suggesting that diffusion plays again an important role in the reaction. At these scan rates, the anodic process increases significantly

indicating the presence of an oxidizable species, with peak current ratios (i_{pc}/i_{pa}) close to 1. This fact suggests that the process approaches the reversibility, which can also be deduced by the minimal shift of the peak potentials (and peak potential difference, ΔE_p), even at the highest scan rates evaluated. The behavior found is typical of a chemical reaction coupled to the reduction of Cu(II) to Cu(I) that regenerates the initial species, a catalytic reaction^{35,34}. At low scan rates, the Cu(I) species reacts rapidly with another species, so it is not available for the anodic reaction in the reverse scan, and, therefore, no anodic currents are observed in the voltammograms. At high scan rates, the coupled reaction appears to be slower than the electrochemical reaction, so the Cu(I) species is available for the re-oxidation, which translates to a peak-shaped response in the voltammogram. Therefore, these studies confirm the presence of a chemical reaction coupled to the electrochemical reaction of Cu(II)/Cu(I). Moreover, as the voltammograms show a quasi-limiting cathodic current for the Cu(II) reduction to Cu(I), it suggests an enhanced mass transfer or a fast regeneration of the initial species, Cu(II). As the measurements are performed in a quiescent solution, the latter case is the most probably: Cu(II) is regenerated in the coupled reaction. At low scan rates, the diffusion layer does not diminish with time as Cu(II) is being regenerated near the electrode surface, the flow of reagent is kept constant and a quasi-limiting current is obtained. At high scan rates, the coupled chemical reaction is not fast enough to regenerate Cu(II), which is depleted over time at the electrode surface. This way, the length of the diffusion layer increases, being necessary to transfer Cu(II) from the bulk solution, a diffusion-controlled process with a peak-based voltammetric response. The Cu(II)/Cu(I) redox couple follows the electrochemical reaction indicated by **equation 1**. The coupled reaction is likely to be the oxidation of Cu(I) by dissolved O₂ in solution as the measurements are conducted in an open atmosphere. Several works have described this reaction (**equation 2**) in ammonia media^{20,21}. Another reaction which could be happening is the disproportionation reaction of Cu(I) to Cu(II) and Cu(0), although some authors mentioned that this reaction has a relatively long induction period because it is endothermic due to Cu(0) lattice energy³⁶. But if this reaction would occur, the generated Cu(0) in ammonia media and

in presence of O₂, usually dissolves to generate Cu(II) as described by **equation 3**^{37,24,25}. Two mechanisms have been proposed for this reaction, at high NH₃ and O₂ concentrations, Cu(0) is oxidized due to the O₂ present in solution following **equation 3**, while that at low concentrations of O₂ and high concentrations of NH₃, Cu(0) oxidation is produced by the reaction of **equation 4**²⁴. New information can be extracted now for the voltammograms at several concentrations of Cu(II) shown in **Figure S1**. On the one hand, the peak current for the ORR decreases generally with increasing concentrations of Cu(II), even though some overlapping with the Cu(I) to Cu(0) process occurred. This fact is due to that while the coupled reaction takes place, the amount of dissolved O₂ decreases and less O₂ is available for the electrochemical ORR. The ORR does not completely disappear even at high Cu(II) concentrations because the solution is in contact with air. On the other hand, the hydrogen evolution reaction (HER), attributed to the cathodic curve at the most negative potentials, increases with increasing concentrations of Cu(II). Cu(0) catalyzes the HER and under these conditions, a greater amount of Cu(0) is available on the electrode surface as suggested by the higher stripping peak currents.



Although it seem clear the presence of the coupled reaction, the magnitudes of the currents obtained can be evaluated in order to see if they deviate significantly from the expected current for a reversible process controlled by diffusion as expected for the Cu(II)/Cu(I) electrochemical reaction in NH₃^{20,21}. **Figure 1C** shows the ratio between the cathodic current obtained experimentally at different scan rates and the expected peak current for a reversible diffusion-controlled process according to the Randles-Sevcik equation for a planar electrode at 25 °C (**equation 5**):

$$i_p = (2.69 \times 10^5) n^{3/2} A C D^{1/2} v^{1/2} \quad (5)$$

where i_p is the peak current intensity (A), n is the number of electrons transferred in the electrochemical reaction, A is the electrode area (cm^2), C is the bulk concentration of the redox species (mol/cm^3), D is the diffusion coefficient of the redox species ($2.1 \times 10^{-5} \text{ cm}^2/\text{s}$) and v is the scan rate (V/s). If the experimental processes follow the reactions in equations 1 and 2, a higher cathodic current compared to the theoretical current is expected for low scan rates because the coupled reaction is capable of regenerating the initial Cu(II) species consuming the Cu(I) species and, therefore, shift the balance of equation 1 towards the products. As shown in the mentioned figure, at these scan rates the deviation between the experimental and theoretical current for a reversible process is greater, while that the current ratio approaches unity at high scan rates. This fact is because the coupled reaction has less influence at high scan rates and the process approaches the reversible reaction schematized in equation 1, controlled by diffusion. These results can also be evaluated by analyzing the chronoamperometric response and comparing with the expected behavior for a process that follows the Cottrell equation (see Supporting Information, **Figure S2**). In order to confirm the influence of the O_2 in the reaction, experiments in absence of oxygen in solution were conducted as described in the experimental section. **Figure S3** shows the voltammograms obtained for a solution of 25 μM of Cu(II) in absence of O_2 in the range of potentials of the Cu(II)/Cu(I) redox couple. As expected, a reversible redox process (with peak potential difference about 80 mV) was obtained for the reaction indicated by equation 1 in absence of O_2 . The peak-shaped response suggests that the mass transfer (diffusion) is limiting the rate of the reaction. The cathodic current is lower than for the same reaction in presence of O_2 , and a notable anodic peak response is also obtained, indicating the availability of Cu(I) for the reverse reaction. Therefore, this study confirms that the main reason for the special voltammetric response of Cu(II)/Cu(I) redox couple obtained previously is the coupled reaction with oxygen from the solution.

It is also interesting to study in more depth the electrochemical processes that occur at the most negative potentials. Voltammograms for a 25 μM solution of Cu(II) in 1 M NH_3 measured at several scan rates were registered and are shown in **Figure 2**. Anodic and cathodic curves are represented separated in order to observe more clearly the processes. At low scan rates, two cathodic processes can be observed (see inset of **Figure 2A**). As described previously, these processes are attributed to the reduction of Cu(I) to Cu(0), and the reduction of dissolved oxygen. Although the Cu(I) reacts with O_2 , a residual amount produced by the reduction of Cu(II) could be present and be reduced at these potentials. Although the cathodic processes are not totally resolved, specially at high scan rates, some information can be extracted from this response, such as the irreversibility of both processes suggested by the shift of the peak potentials with the scan rate. As for the anodic response in this potential range (**Figure 2B**), a stripping process is expected from the oxidation of Cu(0) to Cu(I), with a peak current higher than the reduction process. However, only a small increment in the current (very broad peaks) are observed in these conditions. It seems that the Cu(0) deposited in the cathodic curve disappears before the oxidation can occur in the anodic sweep. Therefore, a coupled reaction also occurs in this case. As described previously, some studies have reported the oxidation of Cu(0) to Cu(II) in NH_3 media, either by dissolved O_2 or by reaction with Cu(II) itself to generate Cu(I) species. At higher concentrations of Cu(II) (**Figure S4**), the stripping process seems to occur in a greater extent than for lower concentrations of Cu(II). This fact indicates that the oxidation of Cu(0) is carried out under these conditions by O_2 , as the expected stripping process is observed confirming the presence of Cu(0). If equation 4 would take place at a significant rate, at higher concentrations of Cu(II), Cu(0) would be also oxidized and the stripping process would be diminished. In order to study these processes in depth, the same voltammograms were recorded in absence of O_2 and are shown in **Figure 2C**. In this case, one cathodic process can be observed in this range of potential, which increases with the copper concentration. Therefore,

this process can be assigned to the reduction of Cu(I) to Cu(0). Although the peak potential of the cathodic process shifted with the copper concentration, it was always below -0.7 V, and therefore, the reduction of Cu(I) to Cu(0) could be tentatively assigned to the first cathodic process appearing in this range of potential in presence of O₂, while that the process at a more negative potential is assigned to the ORR. Regarding the anodic processes, a peak-shaped oxidation response is observed with a significant current, which increases with copper concentration. This process is assigned to the stripping of Cu(0) to Cu(I). In absence of O₂, Cu(0) is electrodeposited in the cathodic sweep and is maintained on the electrode surface. When the appropriate potential is reached, the stripping process is produced, and can be seen even for the lowest copper concentrations evaluated. Therefore, the studies in absence of O₂ confirm that the processes expected for the Cu(I)/Cu(0) redox couple also occur, and that the coupled reaction with O₂ avoids to obtain a defined stripping process in presence of O₂.

[FIGURE 2]

3.2. Electrochemistry of copper at quantum dots-modified screen-printed carbon electrodes

Figure 3 shows the voltammogram obtained for a 25 μM solution of Cu(II) in 1 M NH₃ measured at a scan rate of 50 mV/s using a SPCE modified previously with 4 μL of a 5 nM QDs solution. The potential was swept from +0.5 V to -1.2 V (cathodic curve) and back to the initial potential (anodic curve). In the cathodic curve, two reduction processes can be observed, a process at a potential close to -0.1 V, attributed to the reduction of Cu(II) to Cu(I), and another process at a potential about -0.90 V. This last process is probably a combination of the ORR, which is also observed in the blank solution, and the reduction of Cu(I) to Cu(0), which in this case cannot be differentiated as it was possible at low scan rates for bare SPCEs. The anodic curve is composed by a first oxidation process at a potential near -0.5 V, attributed to the oxidation of Cu(0) to Cu(I) (confirming its previous reduction), and another oxidation process at a potential near 0 V, attributed to the oxidation of Cu(I) to Cu(II). Several significant differences can be observed in the

voltammograms registered under the same conditions at QDs-modified electrodes in comparison to bare SPCEs, also shown in the same figure (and also in **Figure 1A**). Firstly, a lower cathodic current is obtained for the reduction of Cu(II) to Cu(I), while that the peak current of the ORR (although combined with the reduction of Cu(I) to Cu(0)) is significantly higher. These facts suggest that oxygen may be less involved in the coupled reaction. On the one hand, the lower cathodic current and the peak-shape for the Cu(II) to Cu(I) reduction response indicates that Cu(II) is not regenerated as quickly as in bare SPCEs. On the other hand, the higher current observed for the ORR process may suggest that there is a greater amount of O₂ in solution, as it is not reduced in the coupled reaction with Cu(II). Regarding the anodic processes, the greatest differences under these experimental conditions is the significant increment of the oxidation currents for both anodic processes: Cu(0) to Cu(I) and Cu(I) to Cu(II). This fact suggests that there are greater amounts of Cu(0) and Cu(I) available for oxidation when QDs-modified electrodes are used. The blank solution also showed small peaks at a potential near -1 V, which could be tentatively assigned to the cadmium redox processes.

[FIGURE 3]

Similarly to bare SPCEs, the electrochemical behavior of these processes may be more clearly studied using appropriate switching potentials to differentiate both redox couples. Firstly, the processes of Cu(II)/Cu(I) appearing at the most positive potentials were evaluated. **Figure 4A** shows the voltammograms obtained for a 25 μM solution of Cu(II) in 1 M NH₃ measured at several scan rates (0.01-3 V/s) using SPCEs modified with 4 μL of a solution 5 nM of QDs. Interestingly, the voltammograms obtained showed peak-shaped responses for both the cathodic and anodic processes, even at the lowest scan rate applied (5 mV/s). This fact suggests several relevant properties such as that the Cu(I) species electro-generated in the cathodic sweep remains stable for longer times and therefore, its re-oxidation to Cu(II) can be observed in the anodic sweep. The peak-shaped cathodic process shows that the mass transfer of the initial Cu(II) species decreases

with time (and applied potential) as expected for a mass transfer-limiting process since, in this case, the initial Cu(II) is not regenerated by the coupled reaction with O₂. However, the ratio between the experimental peak current and the expected theoretically for a reversible diffusion-controlled process (**Figure 4B**) shows a higher value at low scan rates, with decreasing ratio at increasing scan rates. This fact suggests that the coupled reaction with O₂ is still taking place at some extent, although this ratio is significantly lower at QDs-modified electrodes at low scan rates compared to bare electrodes, suggesting a lower influence of the coupled reaction. At high scan rates, the ratio increases slightly and the values are not as low as those found using bare SPCEs, which were close to 1 (i.e. a higher cathodic current is obtained at QDs-modified electrodes). These results show a difference between what is happening at both electrodes for the cathodic processes. Two main reasons could be the determining factors in this behavior. On the one hand, this curve is plotted using the geometric area as the electrode area, indicating that an increase in the electrode area would lead to increased peak currents. At low scan rates, both electrodes are not comparable because the coupled reaction plays a major role in bare electrodes, but at high scan rates, the coupled reactions should influence to a lesser extent, and the responses should be comparable. On the other hand, adsorption of redox species could lead to the increment in peak currents. **Figure S5** shows the relation between the cathodic peak current and the scan rate (and the square root of the scan rate). A diffusion-controlled process would show linearity between the peak current and the square root of the scan rate and an adsorption-controlled process would be linear with the scan rate. However, the cathodic peak current does not follow total linearity with both parameters, which indicates the influence of other processes. Interestingly, at high scan rates, a linear relation is found between the peak current and the square root of the scan rate, suggesting a diffusion-controlled process when the coupled reaction loss influence. Therefore, it is probably that the higher cathodic peak currents obtained for QDs-modified electrodes in comparison to bare electrodes are due to an increase in the electrode area by the QDs.

[FIGURE 4]

Some information can also be deduced comparing specifically the voltammograms obtained for bare and QDs-modified SPCEs at different scan rates. **Figure 5A** shows the voltammograms at 10 and 2 V/s and **Figure 5B** shows the relationship between the cathodic currents for both electrodes at different scan rates. At low scan rates, the cathodic current is higher using bare electrodes as the coupled oxidation of Cu(I) by O₂ plays a very important role in these electrodes, while in QDs-modified electrodes, although it also occurs, the influence is lower. At certain scan rates, the ratio between the cathodic peak currents approaches unity, while at higher scan rates, the cathodic current obtained using QDs-modified electrodes exceeds that obtained using bare electrodes, probably due to the higher electrode area of QDs-modified electrodes. Regarding the anodic process, the difference in the electrochemical response is even greater. At low scan rates, a small anodic current is obtained using bare electrodes since most of the Cu(I) generated is removed by O₂, although at higher scan rates a peak current is obtained. However, the magnitude of the anodic peak current was significantly higher at the QDs-modified electrodes due to the stabilization of Cu(I). **Figure 6A** shows the relation between the anodic peak current and the scan rate (or the square root of the scan rate). At low scan rates, a strong linearity between the anodic peak current and the scan rate is obtained, suggesting that the adsorption of Cu(I) is the limiting step of the electrochemical reaction, but at high scan rates, the linearity is observed between the peak current and the square root of the scan rate, suggesting a diffusion-controlled process. At these scan rates, the electron transfer between Cu(II)/Cu(I) would take place faster than the adsorption process. The same information can also be deduced comparing the ratio between the anodic and cathodic peak currents for these processes (**Figure 6B**). This ratio is larger than one at low scan rates and decreases with increasing scan rates until be close to unity, suggesting that adsorption plays an important role at low scan rates, as Cu(I) species has enough time to be adsorbed onto the QDs surface. The similar peak currents at high scan rates indicate that similar processes are occurring for the anodic and cathodic reactions, and as adsorption or coupled chemical reactions would have lower influence at

these scan rates, it is probably that diffusion is the limiting step of these reactions. As previously discussed, the cathodic current at high scan rates (and therefore, the anodic current) are significantly higher (~50%) than expected for a diffusion-controlled process (see **Figure 4B**). However, this curve was calculated using the geometric electrode area. These last results seem to confirm that the electroactive area of the QDs-modified electrodes is larger in comparison to bare electrodes, suggested by the higher currents obtained at high scan rates, at which the influence of the coupled processes would be lower. As the quantum dots, with small size and high surface area, play a significant role in the electrochemical reactions, they could increase the electrode area. In essence, these results suggest that the Cu(I) species electro-generated after the reduction of Cu(II) is stabilized by the QDs present on the electrode surface, and their oxidation can be observed clearly at much lower scan rates than for the bare electrode. The stabilization of Cu(I) by the QDs decreases the rate of the reaction indicated by equation 2 (oxidation of Cu(I) by O₂), even using conditions in presence of O₂ and open atmosphere. However, at low scan rates, the coupled chemical reaction still takes place, although at a lesser extent than in bare SPCEs. The stabilization of Cu(I) by QDs is probably due to the adsorption of Cu(I) at the nanocrystal surface and their involvement in the electrochemical processes lead to an increased electrode area. The adsorption of copper species is probably weak as the potential is not shifted significantly between both electrodes.

[FIGURE 5]

[FIGURE 6]

As previously described, in the range of more negative potentials, when QDs-modified electrodes are employed, only one cathodic process can be observed, since both the ORR and the reduction of Cu(II) to Cu(0) appeared at a similar potential. Measurements in this range of potentials were performed in absence of O₂ to confirm the electrochemical processes. **Figure S6** shows a voltammogram obtained for 25 μM Cu(II) in which a cathodic process with E_p near -0.65 V is observed, assigned to the reduction of Cu(II) to Cu(0) and an anodic process with E_p near -0.45 V is

also observed, which is assigned to the stripping of Cu(0) to Cu(I). Although to a lesser extent than in presence of O₂, a small shift of the peak potentials was also observed compared to bare electrodes. The potential shift for the reduction of Cu(I) could be explained as it is being stabilized by the QDs, and the reduction could be slightly more difficult. In addition, as it was previously described, an enhanced stripping process is obtained at QDs-modified electrodes, because Cu(0) can be formed on the surface of QDs by reduction of Cu(I) and the coupled oxidation by O₂ is slower. In order to confirm this fact, electrodeposition of copper (25 μM in 1 M NH₃) was carried out by applying a potential of -1 V for 30 s. Then, the electrodes were washed with ultrapure water and an acid electrolyte (0.1 M H₂SO₄) was employed to study more clearly the stripping of the deposited copper, typically occurring as the oxidation of Cu(0) to Cu(II)²⁸. **Figure S7** shows the voltammograms obtained under the same conditions for bare and QDs-modified electrodes. A stripping process is clearly observed using QDs-modified electrodes, as opposed to bare electrodes, confirming that copper is removed from the carbon surface but remains when QDs are present on the electrode surface.

Finally, a study of the electrodeposition of copper on bare and QDs-modified SPCEs was performed. Electrodeposition was carried out by chronoamperometry using different deposition potentials (-1, -0.8, -0.6 V), Cu(II) concentrations (25, 250 and 2500 μM) and 30 s as deposition time. The chronoamperometric responses were recorded and some of them are shown in **Figure S8**. Neither of the responses fitted perfectly with the typically employed theoretical model proposed by Scharifker-Hills for the two limiting nucleation mechanisms, instantaneous and progressive³⁸, as opposed to the results obtained with the silver electrodeposition on QDs¹⁹. It is likely that other processes are influencing the chronoamperometric response obtained or the nucleation follows a mixed mechanism. Under these conditions, electrodeposition of Cu(0) takes place by the reduction of Cu(I), which is previously generated by reduction of Cu(II). Moreover, as described previously, other coupled processes could happen at the same time (oxidation of Cu(I) or Cu(0) by O₂), and the

ORR also takes place at these potentials. Therefore, all these processes could be influencing the response, and it is not possible to distinguish the response due only to the nucleation and growth of nanoparticles. However, under certain conditions, copper nanoparticles were observed at the electrode surface by SEM. These nanoparticles were relatively small and difficult to detect in most of the electrode surface due to its heterogeneity, roughness and the heterostructure formed by the carbon ink additives. In order to visualize the small nanoparticles by SEM, images were registered for areas of the electrode surface in which large graphite sheets were available. These sheets have a very smooth surface and the nanoparticles can be seen more easily than on the rest of the surface. **Figure 7A-B** shows the SEM micrograph after electrodeposition at -0.8 V for a solution of 250 μM Cu(II) at bare and QDs-modified electrodes. For QDs-modified electrodes, nanoparticles with average size of 31 ± 4 nm were observed, but for the bare electrodes, copper nanoparticles were not observed along the electrode surface, even on the accessible graphite sheets. For bare electrodes, it was necessary to apply a potential of at least -1 V to find deposited copper nanoparticles of around 31 ± 6 nm (**Figure 7C**). Under these conditions the amount/size of nanoparticles is enough to avoid their complete dissolution due to the oxidation with O_2 . A more negative potential could help by depositing a higher amount of copper and also by decreasing the O_2 local concentration by electro-reduction avoiding a quick dissolution of Cu(0). However, it seems that the surface coverage in this case (estimated approximately from the SEM images as 7×10^9 NPs/ cm^2) is lower compared to QDs-modified electrodes (1.4×10^{10} NPs/ cm^2), and a good proportion of them are deposited on the sheet edges and to a lesser extent on the rest of the graphite sheet. The higher electrochemical activity of graphite sheets, with higher ratio of step edges, is currently a highly-discussed research topic³⁹. In some cases, authors propose that the zones of the graphite sheets with small density of defects are electrochemically inert^{40,41}, although a similar electrochemical activity have been found at basal planes, with smaller density of defects, using high-resolution scanning techniques^{42,43}. In our case, although some nanoparticles also appeared on the top of the graphite sheet (probably with lower density of defects), a larger density of nanoparticles were electrodeposited on the edges as seen in

the images. Using Cu(II) concentrations significantly lower (25 μM) and a deposition potential of -1 V, copper nanoparticles were not detected even in the accessible graphite sheets at bare electrodes (**Figure S9A**), suggesting that the small deposited amount of copper is completely and quickly oxidized by O_2 . At QDs-modified electrodes, nanoparticles of 28 ± 3 nm are observed in the graphitic sheets all over their entire surface (**Figure S9B**), without special preference for the sheet edges. This fact suggests that even using low amounts of copper, deposited nanoparticles are observed due to the stabilization of Cu(I) and Cu(0) by the QDs. In addition, the deposition is not preferential to the sheet edges, as happens at bare electrodes, suggesting that the QDs play a decisive role in the formed nanoparticles, and copper could be deposited on the surface of QDs, alike has been described for silver¹⁹. Electrodeposition of metals at QDs-modified electrodes could be a good method in order to avoid the preferential deposition at step edges of screen-printed graphite electrodes as has been reported previously^{44,45}, and be used for the generation of nanostructured electrodes with interesting electrochemical properties.

[FIGURE 7]

4. CONCLUSIONS

This work describes the different electrochemical behavior of copper species in ammonia medium using bare screen-printed carbon electrodes and modified with CdSe/ZnS quantum dots. We have found that the presence of quantum dots on the electrode surface stabilizes the electro-generated copper species, Cu(I) and Cu(0), while that in absence of quantum dots, the oxidation of these species to Cu(II) takes place by action of the dissolved oxygen in the solution. There seems to be some interaction between the copper species and quantum dots, probably a weak adsorption, which is the main cause for the stabilization. Electrodeposition studies followed by electron microscopy showed that, under some conditions, copper nanoparticles are deposited on the electrode surface if quantum dots are available, but they disappear when are deposited on bare carbon electrodes. This

study shows how the quantum dots can modify the behavior of different electroactive species, and could be useful for the random deposition of nanoparticles on electrodes avoiding the electrodeposition only onto the most active electrode areas.

ASSOCIATED CONTENT

Supporting Information

Figures displaying some electrochemical measurements of copper at bare and quantum-dots modified electrodes and chronoamperometric responses and SEM images of the electrode surface after copper electrodeposition.

AUTHOR INFORMATION

Corresponding Author

*E-mail: costa@uniovi.es (A. Costa-García).

Notes

The authors declare no competing financial interest.

ACKNOWLEDGEMENTS

This work has been supported by the FC-15-GRUPIN-021 project from the Asturias Regional Government and the CTQ2014-58826-R project from the Spanish Ministry of Economy and Competitiveness (MEC). Daniel Martín-Yerga thanks the MEC for the award of a FPI grant (BES-2012-054408).

REFERENCES

1. A. P. Alivisatos, *Science* (80-.), 1996, **271**, 933–937.
2. S. K. Haram, A. Kshirsagar, Y. D. Gujarathi, P. P. Ingole, O. A. Nene, G. B. Markad, and S. P. . Nanavati, *J. Phys. Chem. C*, 2011, **115**, 6243–6249.
3. M. Amelia, S. Impellizzeri, S. Monaco, I. Yildiz, S. Silvi, F. M. Raymo, and A. Credi,

- ChemPhysChem*, 2011, **12**, 2280–2288.
4. A. J. Nozik, M. C. Beard, J. M. Luther, M. Law, R. J. Ellingson, and J. C. Johnson, *Chem. Rev.*, 2010, **110**, 6873–6890.
 5. R. Gill, M. Zayats, and I. Willner, *Angew. Chemie Int. Ed.*, 2008, **47**, 7602–7625.
 6. S. K. Haram, B. M. Quinn, and a J. Bard, *J. Am. Chem. Soc.*, 2001, **123**, 8860–8861.
 7. M. Amelia, C. Lincheneau, S. Silvi, and A. Credi, *Chem. Soc. Rev.*, 2012, **41**, 5728.
 8. F. Lisdat, D. Schäfer, and A. Kapp, *Anal. Bioanal. Chem.*, 2013, **405**, 3739–3752.
 9. W.-W. Zhao, J. Wang, Y.-C. Zhu, J.-J. Xu, and H.-Y. Chen, *Anal. Chem.*, 2015, **87**, 9520–9531.
 10. M. Roushani and Z. Abdi, *Sens. Actuators B*, 2014, **201**, 503–510.
 11. F. Shahdost-fard and M. Roushani, *J. Electroanal. Chem.*, 2016, **763**, 18–24.
 12. D. Martín-Yerga, M. B. González-García, and A. Costa-García, *Talanta*, 2014, **130**, 598–602.
 13. D. Martín-Yerga and A. Costa-García, *Bioelectrochemistry*, 2015, **105**, 88–94.
 14. J. Yao, S. Schachermeyer, Y. Yin, and W. Zhong, *Anal. Chem.*, 2011, **83**, 402–408.
 15. K. Huang, K. Xu, J. Tang, L. Yang, J. Zhou, X. Hou, and C. Zheng, *Anal. Chem.*, 2015, **87**, 6584–6591.
 16. D. H. Son, S. M. Hughes, Y. Yin, and A. P. Alivisatos, *Science (80-.)*, 2004, **306**, 1009–1012.
 17. B. J. Beberwyck, Y. Surendranath, and A. P. Alivisatos, *J. Phys. Chem. C*, 2013, **117**, 19759–19770.
 18. J. B. Rivest and P. K. Jain, *Chem. Soc. Rev.*, 2013, 89–96.
 19. D. Martín-Yerga, E. C. Rama, and A. Costa-García, *Anal. Chem.*, 2016, **88**, 3739–3746.
 20. A. Darchen, R. Drissi-Daoudi, and A. Irzho, *J. Appl. Electrochem.*, 1997, **27**, 448–454.
 21. R. Drissi-Daoudi, A. Irzho, and A. Darchen, *J. Appl. Electrochem.*, 2003, **33**, 339–343.
 22. J. Halpern, .
 23. B. C.-Y. Lu and W. F. Graydon, *J. Am. Chem. Soc.*, 1955, **77**, 6136–6139.
 24. F. Habashi, *Berichte der Bunsengesellschaft für Phys. Chemie*, 1963, **67**, 402–406.
 25. Q. Luo, R. A. Mackay, and S. V Babu, *Chem. Mater.*, 1997, **9**, 2101–2106.
 26. C. Nila and I. González, *J. Electroanal. Chem.*, 1996, **401**, 171–182.
 27. A. Ramos, M. Miranda-Hernández, and I. González, *J. Electrochem. Soc.*, 2001, **148**, C315.
 28. D. Grujicic and B. Pesic, *Electrochim. Acta*, 2002, **47**, 2901–2912.
 29. D. Grujicic and B. Pesic, *Electrochim. Acta*, 2005, **50**, 4426–4443.
 30. S. J. Figueroa-Ramírez and M. Miranda-Hernández, *ECS Trans.*, 2009, **20**, 345–355.
 31. L. Dai, Y. Xue, L. Qu, H.-J. Choi, and J.-B. Baek, *Chem. Rev.*, 2015, **115**, 4823–4892.
 32. T. F. Braish, R. E. Duncan, J. J. Harber, R. L. Steffen, and K. L. Stevenson, *Inorg. Chem.*, 1984, **23**, 4072–4075.
 33. J. Bjerrum, S. Pajunen, G. Lindblom, K. Fontell, C. J. Nielsen, F. Urso, J. Weidlein, and R. A. Zingaro, *Acta Chem. Scand.*, 1986, 40a, 233–235.
 34. A. J. Bard and L. R. Faulkner, *Electrochemical Methods - Fundamentals and Applications*, John Wiley & Sons, 2nd Edition., 2001.
 35. T. J. Zerk and P. V Bernhardt, *Dalt. Trans.*, 2013, **42**, 11683.
 36. A. Burg and D. Meyerstein, *The chemistry of monovalent copper in aqueous solutions*, ., 1st edn., 2012, vol. 64.
 37. D. Strmčnik, M. Gaberšček, B. Pihlar, D. Kočar, and J. Jamnik, *J. Electrochem. Soc.*, 2009, **156**, C222.
 38. B. Scharifker and G. Hills, *Electrochim. Acta*, 1983, **28**, 879–889.

39. R. L. McCreery and M. T. McDermott, *Anal. Chem.*, 2012, **84**, 2602–2605.
40. C. E. Banks, T. J. Davies, G. G. Wildgoose, and R. G. Compton, *Chem. Commun. (Camb.)*, 2005, 829–841.
41. N. A. Choudry, D. K. Kampouris, R. O. Kadara, and C. E. Banks, *Electrochem. commun.*, 2010, **12**, 6–9.
42. S. C. S. Lai, A. N. Patel, K. McKelvey, and P. R. Unwin, *Angew. Chem. Int. Ed. Engl.*, 2012, **51**, 5405–8.
43. A. N. Patel, M. G. Collignon, M. a O'Connell, W. O. Y. Hung, K. McKelvey, J. V Macpherson, and P. R. Unwin, *J. Am. Chem. Soc.*, 2012, **134**, 20117–30.
44. N. A. Choudhry, R. O. Kadara, N. Jenkinson, and C. E. Banks, *Electrochem. commun.*, 2010, **12**, 406–409.
45. S. J. Rowley-Neale, D. A. C. Brownson, and C. E. Banks, *Nanoscale*, 2016, **8**, 15241–15251.

FIGURES

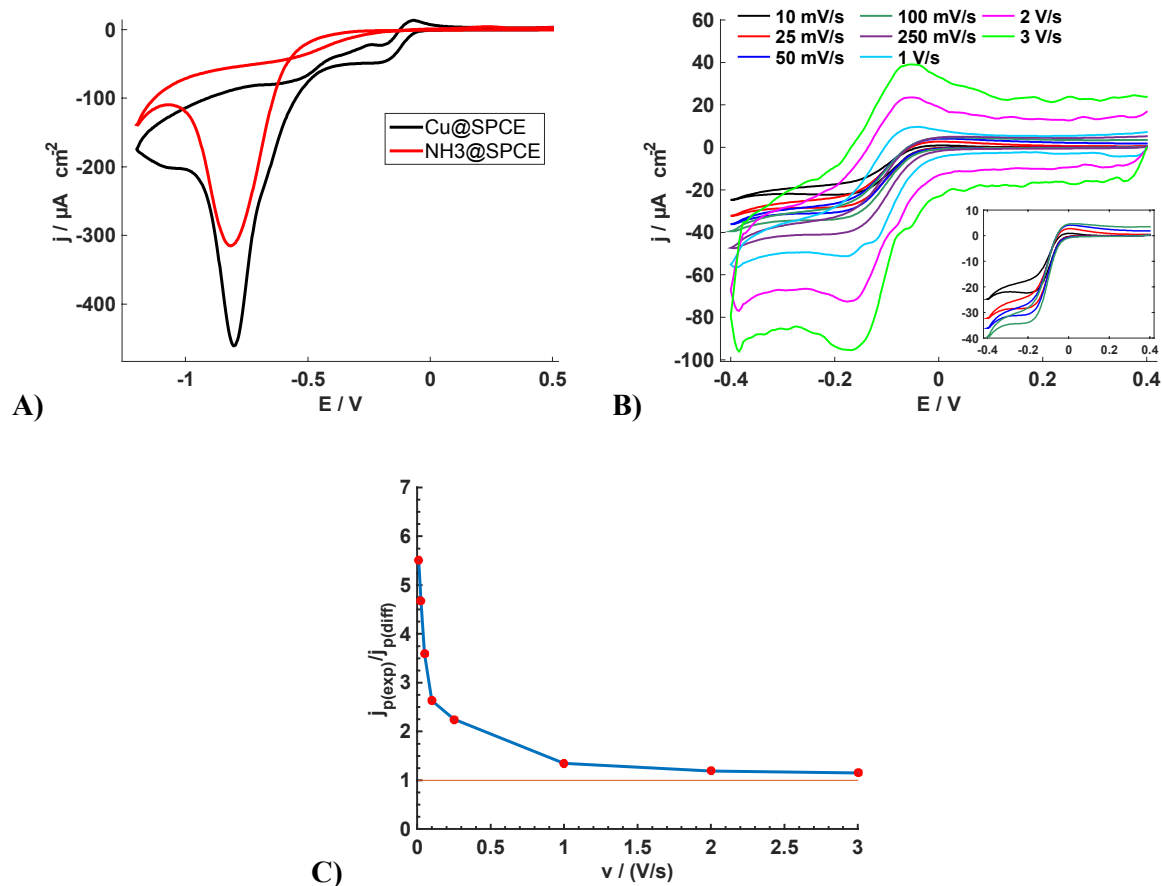


Figure 1. A) Cyclic voltammograms at 50 mV/s of a solution containing 25 μM of Cu(II) in 1 M NH₃ (black line) and blank (red line) at bare screen-printed electrodes. B) Cyclic voltammograms at several scan rates from +0.4 to -0.4 V of a solution containing 25 μM of Cu(II) in 1 M NH₃ at bare electrodes. Inset:

voltammograms at the lowest scan rates (10-100 mV/s). C) Variation of the ratio between the experimental cathodic peak current and the expected for a diffusion-controlled process with the scan rate. Data obtained from cyclic voltammograms of 25 μM Cu(II) at bare electrodes.

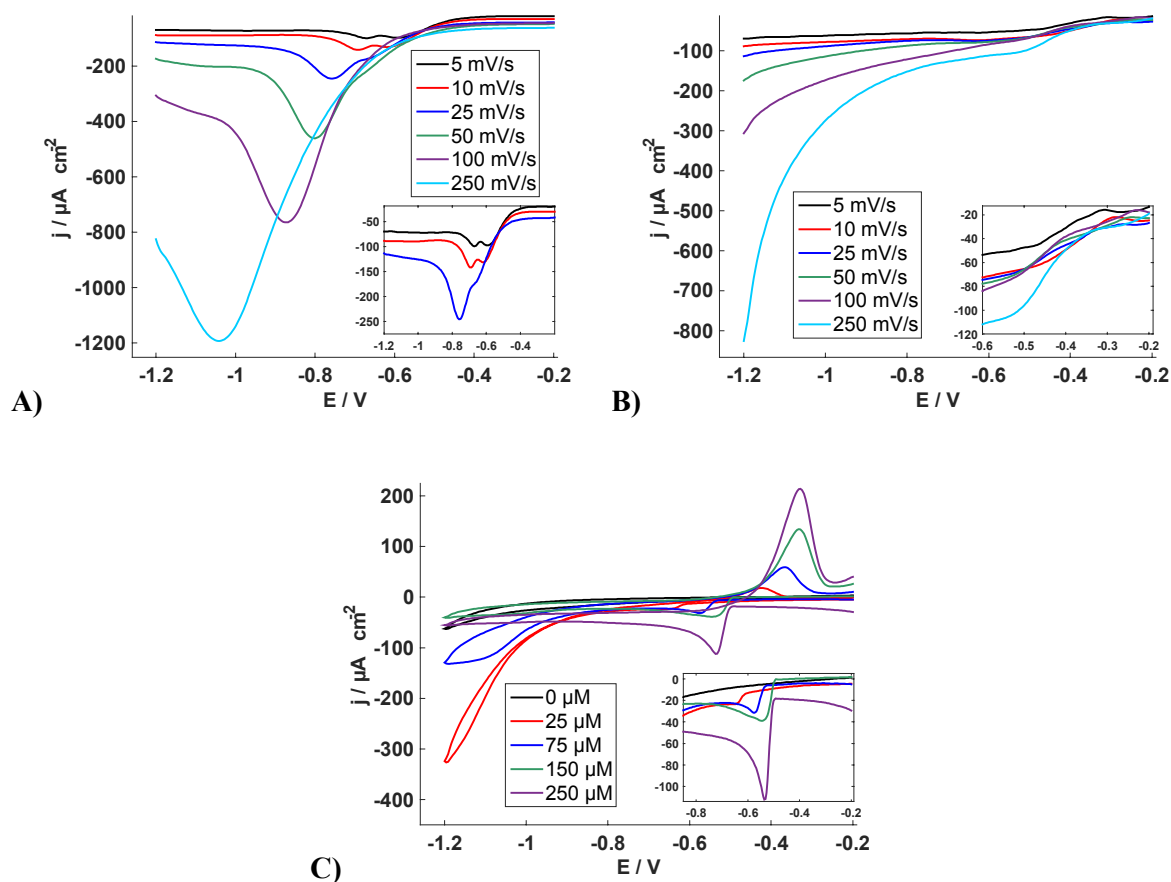


Figure 2. A) Cathodic curve of the cyclic voltammograms from -0.2 to -1.2 V obtained for a solution of 25 μM at several scan rates using bare electrodes. Inset shows the curves for the lowest scan rates (5, 10, 25 mV/s). B) Anodic curve of the cyclic voltammograms from -0.2 to -1.2 V obtained for a solution of 25 μM at several scan rates using bare electrodes. Inset shows the curves in the range of potentials where the copper stripping appears. C) Cyclic voltammograms at 50 mV/s from -0.2 to -1.2 V obtained for solutions containing 0, 25, 75, 150 and 250 μM of Cu(II) using bare electrodes in absence of oxygen.

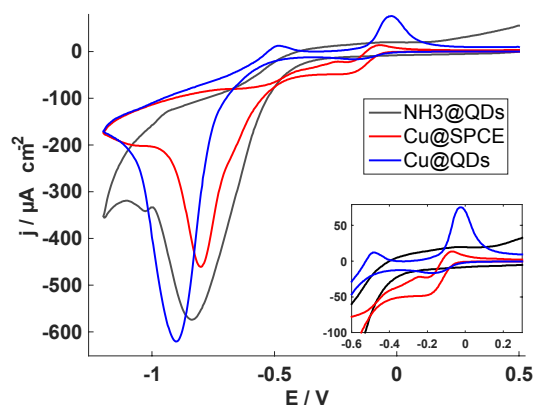


Figure 3. Cyclic voltammograms at 50 mV/s from +0.5 to -1.2 V for a solution containing 25 μM of Cu(II) in 1 M NH_3 using bare electrodes (red line) and QDs-modified electrodes (blue line). Black line shows the voltammogram obtained at the same conditions for a solution containing 1 M NH_3 .

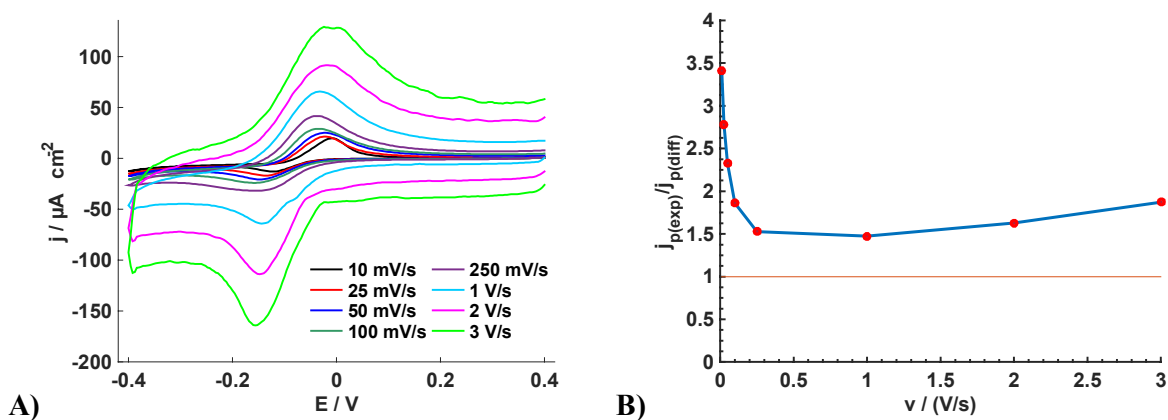


Figure 4. **A)** Cyclic voltammograms from +0.4 to -0.4 V for a solution containing 25 μM of Cu(II) at several scan rates using QDs-modified electrodes. **B)** Variation of the ratio between the experimental cathodic peak current and the expected for a diffusion-controlled process with the scan rate. Data obtained from cyclic voltammograms of 25 μM Cu(II) at QDs-modified electrodes.

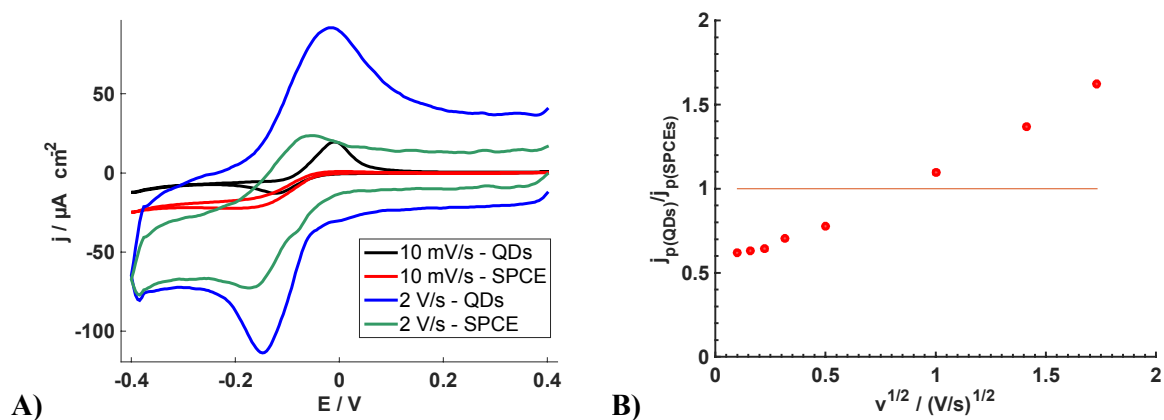


Figure 5. A) Cyclic voltammograms from +0.4 to -0.4 V for a solution containing 25 μM of Cu(II) at several scan rates using bare and QDs-modified electrodes. B) Variation of the ratio between the cathodic peak current obtained at QDs-modified electrodes and bare electrodes with the scan rate.

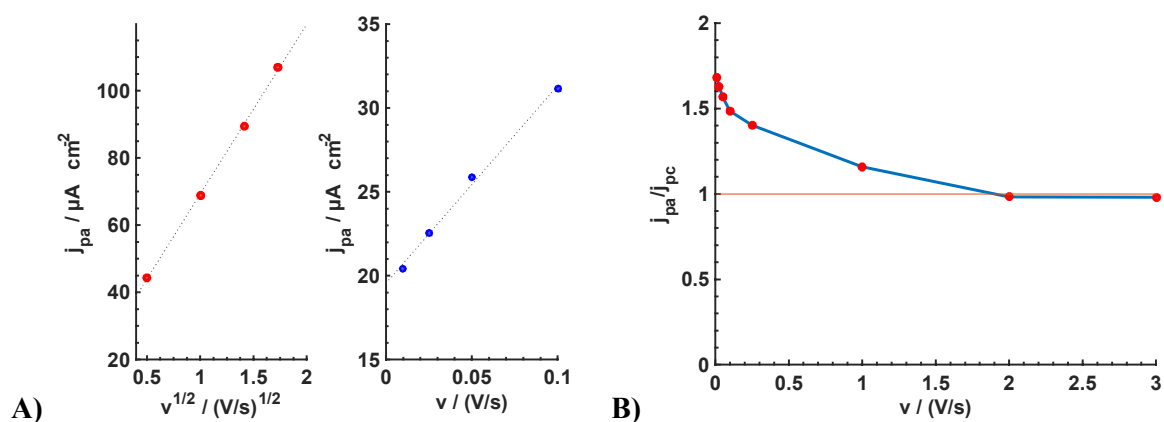


Figure 6. A) Relationship between the anodic peak current obtained at QDs-modified electrodes and the square root of the scan rate (at high scan rates) and relationship between the anodic peak current obtained at QDs-modified electrodes and the scan rate (at low scan rates). B) Variation of the ratio between the anodic and cathodic peak currents obtained at QDs-modified electrodes with the scan rate.

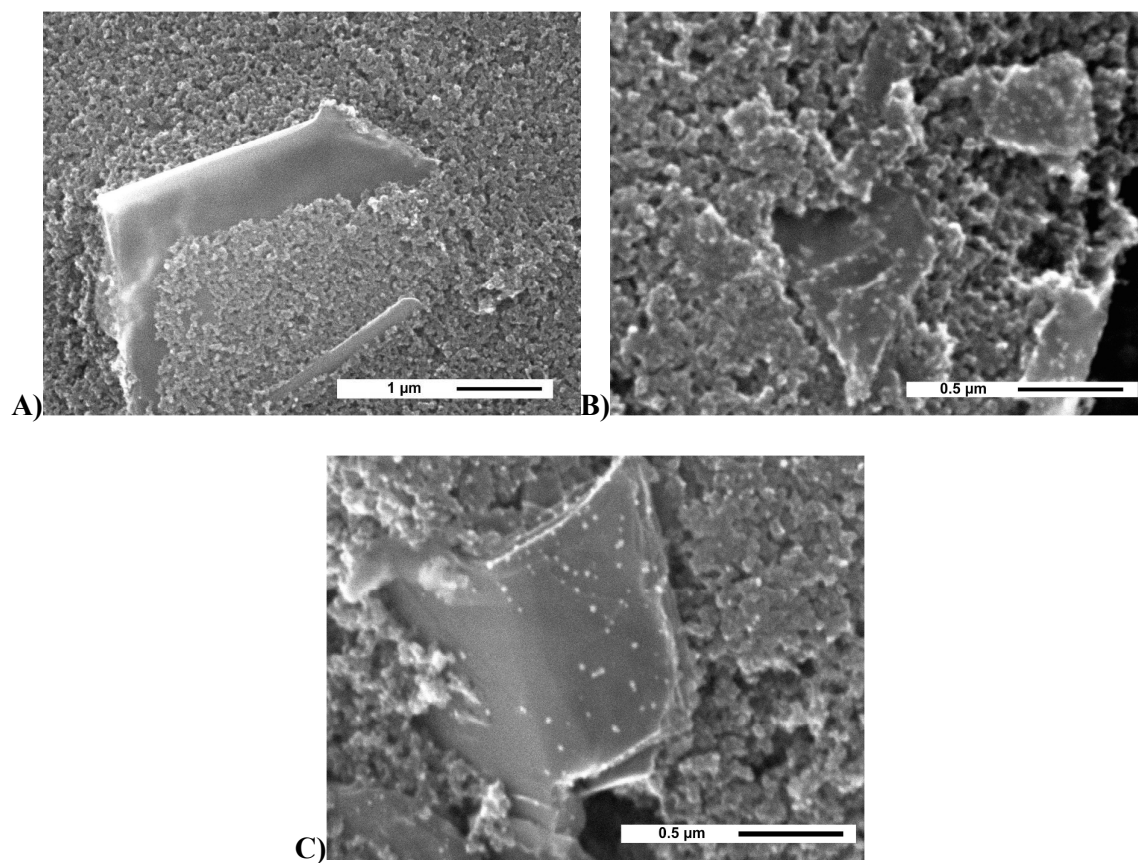


Figure 7. **A)** SEM micrograph of the electrode surface after electrodeposition of 250 μM of Cu(II) in 1 M NH_3 at -0.8 V for 30 s at bare electrodes. **B)** SEM micrograph of the electrode surface after electrodeposition of 250 μM of Cu(II) in 1 M NH_3 at -0.8 V for 30 s at QDs-modified electrodes. **C)** SEM micrograph of the electrode surface after electrodeposition of 250 μM of Cu(II) in 1 M NH_3 at -1 V for 30 s at bare electrodes.

SUPPORTING INFORMATION**Stabilization of Electrogenenerated Copper Species on Electrodes
Modified with Quantum Dots**

*Daniel Martín-Yerga and Agustín Costa-García**

Departamento de Química Física y Analítica, Universidad de Oviedo, 33006 Oviedo, Spain.

*E-mail: costa@uniovi.es

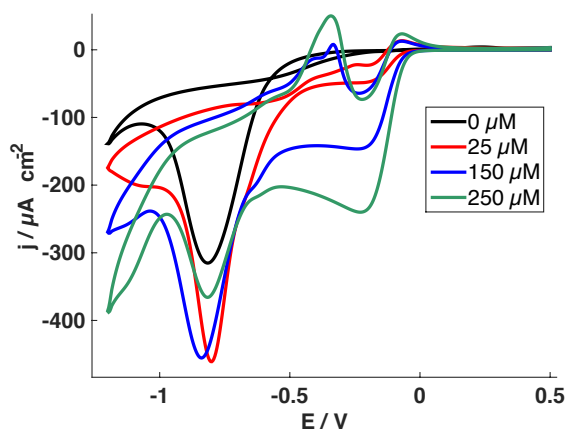


Figure S1. Cyclic voltammograms at 50 mV/s of solutions containing 0, 25, 150 or 250 μM of Cu(II) in 1 M NH_3 at bare electrodes.

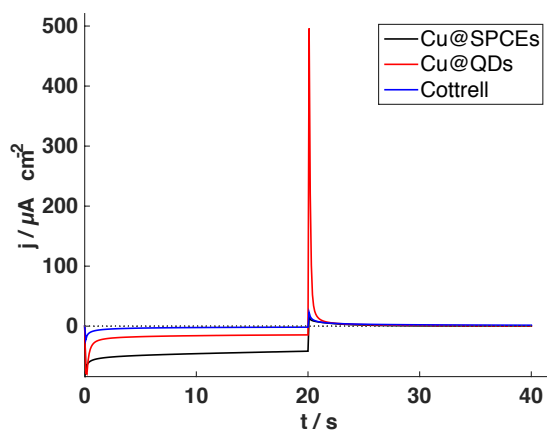


Figure S2. Chronoamperometric responses obtained for a solution of 25 μM Cu(II) in 1 M NH_3 after applying -0.3 V and +0.05 V for 20 s at bare SPCEs (black line), QDs-modified SPCEs (red line) and expected response for a diffusion-controlled process following the Cottrell equation (blue line). The cathodic current obtained at bare SPCEs is significantly higher than at QDs-modified electrodes or for a diffusion-controlled process due to the influence of the coupled chemical reaction regenerating the initial species. Both responses were higher than the expected Cottrell response. The subsequent anodic current obtained at QDs-modified electrodes was significantly higher as more Cu(I) was available for the oxidation due to the stabilization by QDs. The anodic response at bare SPCEs was slightly lower than the Cottrell response, as a small amount of Cu(I) is available due to the previous oxidation with O_2 . The Cottrell equation is as follows:

$$j = n F D^{1/2} C \pi^{-1/2} t^{-1/2},$$

where j is the current density, n is the number of electrons exchanged, D is the diffusion coefficient of the electroactive species, C is the initial concentration of the electroactive species and t is the time of experiment.

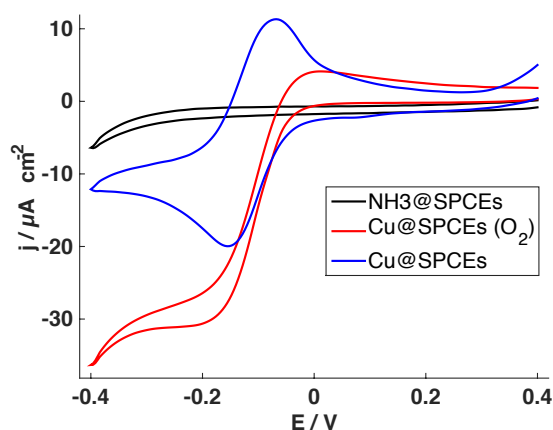


Figure S3. Cyclic voltammograms at 50 mV/s from +0.4 to -0.4 V obtained for a 25 μM Cu(II) solution in presence of O₂ (red line) and absence of O₂ (blue line) and voltammogram for the blank solution in absence of O₂ (black line).

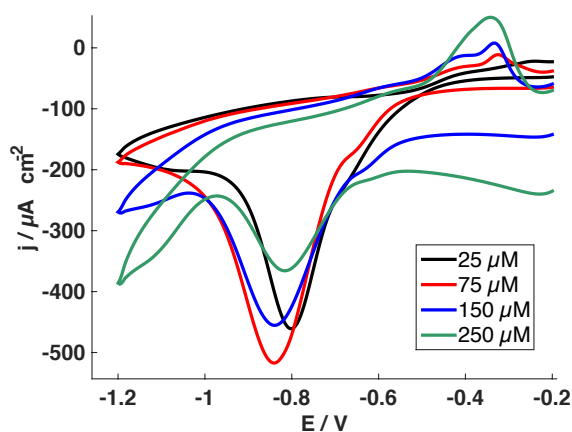


Figure S4. Cyclic voltammograms at 50 mV/s from -0.2 to -1.2 V obtained for solutions of 25, 75, 150 and 250 μM of Cu(II) using bare electrodes.

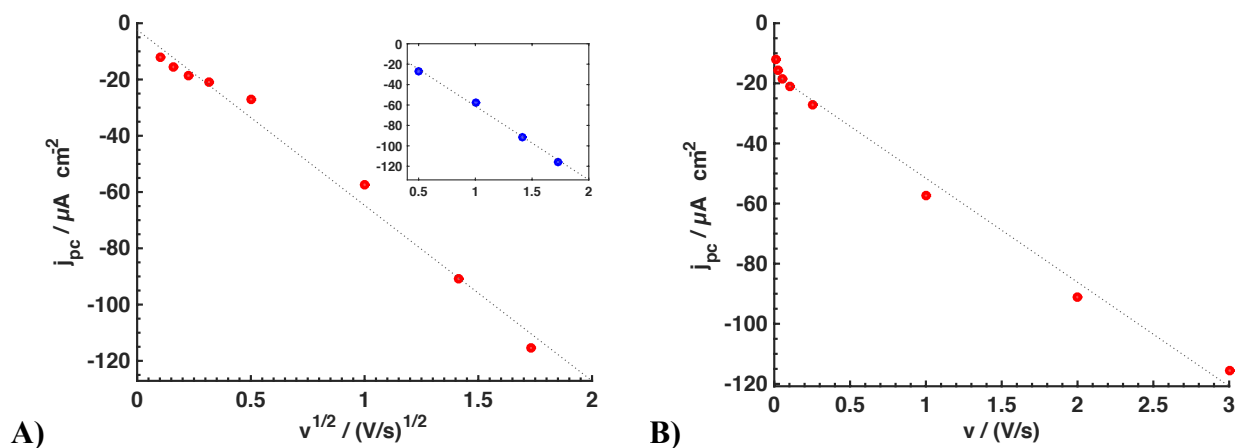


Figure S5. A) Relationship between the cathodic peak current obtained at QDs-modified electrodes and the square root of the scan rate. Inset: same plot for the highest scan rates (0.25-3 V/s) showing their linear relationship. B) Relationship between the cathodic peak current obtained at QDs-modified electrodes and the scan rate.

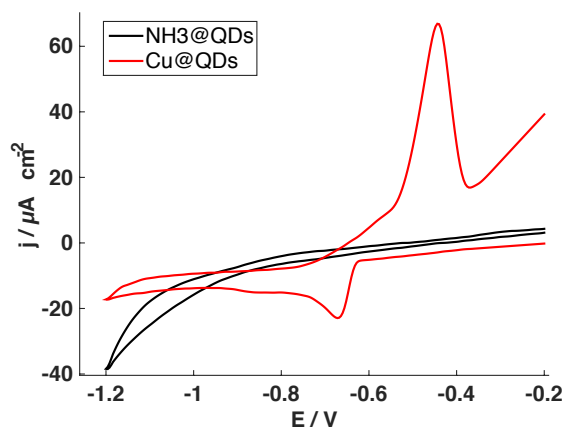


Figure S6. Cyclic voltammograms at 50 mV/s from -0.2 to -1.2 V obtained for a solution of 25 μM of Cu(II) (red line) and blank (black line) at QDs-modified electrodes in absence of oxygen.

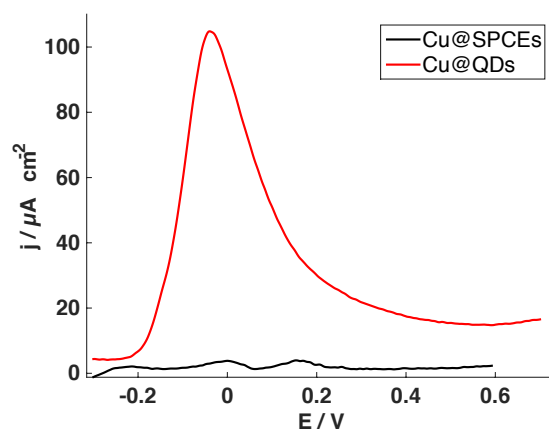


Figure S7. Linear-sweep anodic stripping voltammograms obtained in 0.1 M H_2SO_4 for bare and QDs-modified electrodes after electrodeposition at -1 V for 30 s of a solution of 25 μM of Cu(II) in 1 M NH_3 and washing with ultrapure water.

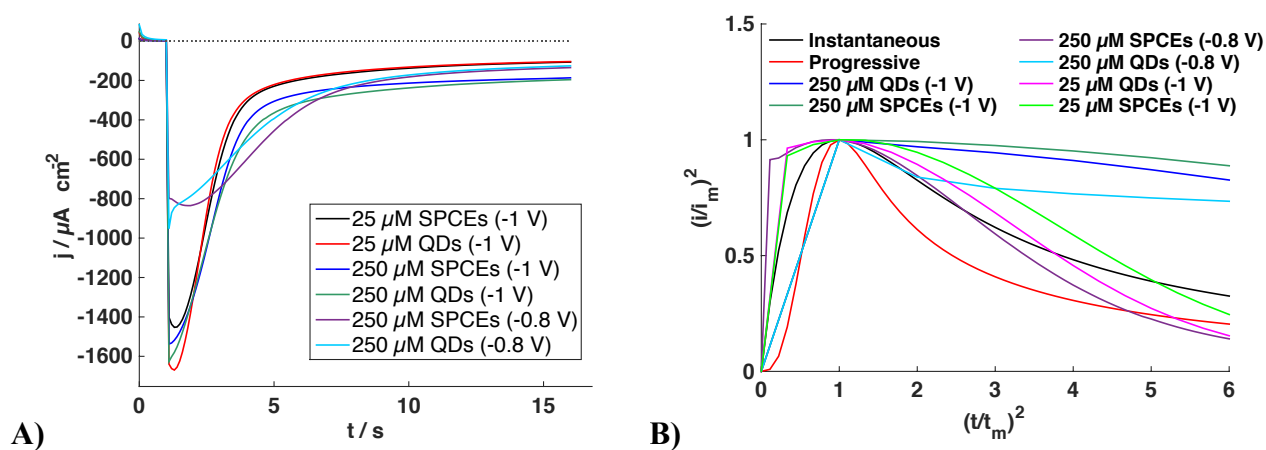


Figure S8. A) Chronoamperometric responses for the electrodeposition of copper in 1 M NH_3 at bare and QDs-modified electrodes under different experimental conditions. B) Scharifker-Hills model i - t transients for the electrodeposition of copper at bare and QDs-modified electrodes under different experimental conditions.

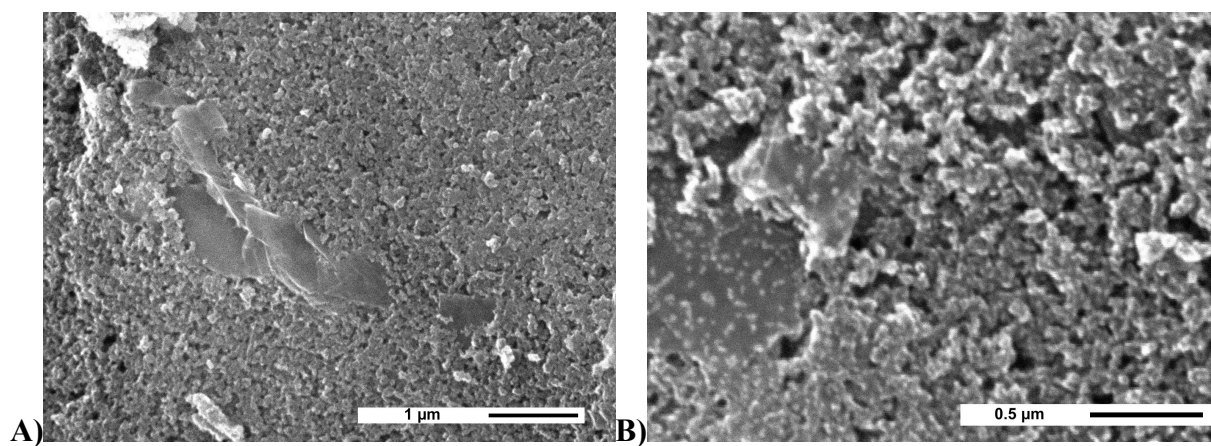


Figure S9. **A)** SEM micrograph of the electrode surface after electrodeposition of 25 μM of $\text{Cu}(\text{II})$ in 1 M NH_3 at -1 V for 30 s at bare electrodes. **B)** SEM micrograph of the electrode surface after electrodeposition of 25 μM of $\text{Cu}(\text{II})$ in 1 M NH_3 at -1 V for 30 s at QDs-modified electrodes.